

Original Article

Cite this article: Zhang Q, Chen Y, Fang D, Iannuzzi C, and Klein E. (2023) Evaluation of the accuracy of a six-degree-of-freedom robotic couch using optical surface and cone beam CT images of an SRS QA phantom. *Journal of Radiotherapy in Practice*. **22**(e69), 1–5. doi: [10.1017/S1460396922000395](https://doi.org/10.1017/S1460396922000395)

Received: 5 July 2022

Revised: 1 December 2022

Accepted: 1 December 2022

Key words:


6-DOF couch; CBCT; Vision RT

Author for correspondence:

Qinghui Zhang, Department of Oncology, Saint Vincent's Medical Center, Bridgeport, CT 06606, USA.

E-mail: Qinghui.zhang@gmail.com

Evaluation of the accuracy of a six-degree-of-freedom robotic couch using optical surface and cone beam CT images of an SRS QA phantom

Q. Zhang¹ , Y. Chen², D. Fang¹, C. Iannuzzi¹ and E. Klein³

¹Department of Oncology, Saint Vincent's Medical Center, Bridgeport, CT 06606, USA; ²Department of Radiation Medicine, Lombardi Comprehensive Cancer Center, MedStar Georgetown University Hospital, Washington, DC 20007, USA and ³Department of Radiation Oncology, Brown Alpert Medical School, Providence, RI 02903, USA

Abstract

Purpose: To assess the accuracy of the Varian PerfectPitch six-degree-of-freedom (6DOF) robotic couch by using a Varian SRS QA phantom.

Methods: The stereotactic radiosurgery (SRS) phantom has five tungsten carbide BBs each with 7.5 mm in diameter arranged with the known geometry. Optical surface images and cone beam CT (CBCT) images of the phantom were taken at different pitch, roll and rotation angles. The pitch, roll, and rotation angles were varied from -3 to 3 degrees by inputs from the linac console. A total of 39 Vision RT images with different rotation angle combinations were collected, and the Vision RT software was used to determine the rotation angles and translational shifts from those images. Eight CBCT images at most allowed rotational angles were analysed by in-house software. The software took the coordinates of the voxel of the maximum CT number inside a 7.5-mm sphere surrounding one BB to be the measured position of this BB. Expected BB positions at different rotation angles were determined by multiplying measured BB positions at zero pitch and roll values by a rotation matrix. Applying the rotation matrix to 5 BB positions yielded 15 equations. A linear least square method was used for regression analysis to approximate the solutions of those equations.

Results: Of the eight calculations from CBCT images, the maximum rotation angle differences (degree) were 0.10 for pitch, 0.15 for roll and 0.09 for yaw. The maximum translation differences were 0.3 mm in the left–right direction, 0.5 mm in the anterior–posterior direction and 0.4 mm in the superior–inferior direction.

Conclusions: The uncertainties of the 6-DOF couch were examined with the methods of optical surface imaging and CBCT imaging of the SRS QA phantom. The rotational errors were less than 0.2 degree, and the isocentre shifts were less than 0.8 mm.

Introduction

Rotational errors always exist in set-up processes during radiation therapy treatment, introducing extra clinical target volume and planning target volume margins and dosimetry errors.^{1–10} Different kinds of six-degree-of-freedom (6-DOF) couches have been utilised to correct rotational errors.^{11–16} The Varian 6-DOF PerfectPitch robotic couch recently introduced to clinic by Varian (Varian Medical Systems, Palo Alto, CA, USA) can compensate for such errors if detected.^{17–20}

Cone beam CT (CBCT) is a standard method used in patient set-up. By registration of patient's set-up CBCT and planning CT images, translational and rotational errors can be determined.^{21–25} Besides CBCT, AlignRT (Vision RT, London, UK) is a video-based 3D optical surface imaging system which has been widely applied in radiation therapy.^{26–32} AlignRT acquires and registers patient's optical surface images before and during treatment with the reference surface image generated through the same patient's 3D planning CT image in order to monitor patient organ/tissue motion in the course of treatment. It has been used for treatment set-up and monitoring for stereotactic radiosurgery (SRS), stereotactic body radiotherapy (SBRT) and breast patients.

Vision RT can also be used for gating treatments. For breast treatments, Vision RT and deep inspiration breath-hold patients normally receive less dose to heart.^{31,33}

Vision RT and CBCT are two standard methods for patient set-up in Edge™ Radiosurgery System (Varian). We compare the accuracy of the two methods in detection for SRS and SBRT patients.

In Ref. 18, the authors tested a new methodology for rotational accuracy assessment. This method is fully adaptable to clinical usage using Varian's IsoCal phantom (Varian Medical

Table 1. Position index of the five BBs in the SRS phantom. When one faces the machine, X direction is from left to right and positive Y direction is towards machine and positive Z direction towards ceiling. Sphere positions listed are respect to the centre of the phantom which is also the centre of sphere 3 when the phantom is correctly positioned in the machine system

BB index	X(mm)	Y(mm)	Z(mm)
1	-25	-10	-30
2	-15	+10	-15
3	0	0	0
4	+20	-20	+10
5	+30	20	+20

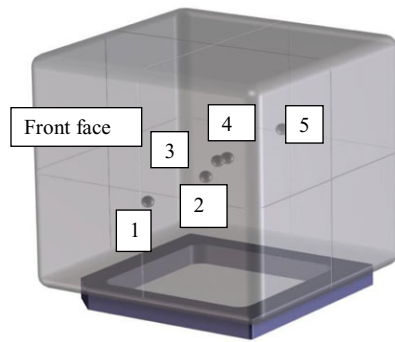


Figure 1. Arrangement of the five BBs inside the SRS phantom.

Systems, Palo Alto, CA, USA) which was designed for isocentre calibration.^{34,35} The 3D kV CBCT scans of IsoCal phantom were used and registered to CBCT image at neutral positions. By registration of 16 tungsten carbide BBs with known geometry inside IsoCal phantom at different rotational angles, the authors found that the accuracy level of Varian 6-DOF PerfectPitch couch is sufficient for patient treatments.

We used the method described in the previous publication²¹ to detect the BBs inside an SRS phantom and to register those BBs at different rotational angles to estimate the rotation angles. By comparing the calculation results between CBCT and Vision RT, the accuracy of the Vision RT was evaluated.

Materials and Methods

SRS phantom and 6DOF of couch

The Varian SRS phantom is a cube with a side length of 15 cm. There are five tungsten carbide BBs inside the phantom, each with 7.5 mm in diameter, arranged in a known geometry and specifically designed for imaging isocentre calibration. The five BB positions are given in Table 1.

Detailed information about this phantom's usage can be found in reference.³⁶ The Varian SRS phantom and its five BBs positions inside the phantom are displayed in Figure 1.

The PerfectPitch couch from Varian was used in this study. This couch can be rotated with a combination of known yaw, pitch and roll angles.

Table 2. List of equations used in this paper

Equation index	Explanation
Eq. (1)	The expression of the rotation matrix
Eq. (2)	The expression of the translation matrix
Eq. (3)	The relationship between CBCT images and CT images
Eq. (4)	The quantity to be minimised by the linear square method
Eq. (5)	A solution of the translation matrix
Eq. (6)	A solution of the rotation matrix
Eq. (7)	The singular value decomposition of the matrix

Determination of the BBs' positions inside the SRS phantom

Moving a sphere of 7.5 mm diameter in the CBCT image, when the sum of the CT numbers inside this sphere reached a maximum, the sphere was assumed to coincide with a BB. The centre of this sphere was defined as the position for this BB. All five BBs positions were determined in this way. The centre of the third BB was defined as the isocentre of the mechanical system according to the phantom design.

From the console, different couch rotation angles were input. A CBCT image was taken for each combination of rotation angles. The BBs positions were determined using the method given above. By using a rotation matrix and a translation matrix, the different positions of five BBs at different angles can be linked to their initial positions where all rotational angles were zeros. Consequently, a rigid transformation with rotations and translations can be estimated. Therefore, differences of three rotational angles between the console input values and calculated values can be determined. Those differences were taken as the residual errors of the system.

The coordinate system

The laboratory coordinate system definition by Siddon et al.³⁷ was used in this study. The origin of the laboratory coordinate system is the isocentre of the linear accelerator. The X_{Lab} axis directed to the viewer's right when facing the gantry, the Y_{Lab} directed from the isocentre towards the gantry and the Z_{Lab} directed upwards from the isocentre. The α , β and γ denote pitch, roll and yaw, respectively. Those three rotations are around X, Y and Z directions. The rotated coordinate system was named as the experimental system, and the three axes were labelled as X_T , Y_T and Z_T . In the following, seven equations were introduced and used in data analyses. A list of those equations and their explanations are given in Table 2.

The experimental coordinate system was determined by matching the CBCT images with the planning CT images. There are N (which is 5 in this publication) small BBs with the coordinate values of $\vec{V}_{CT}(i)$, $i = 1, 2, 3, \dots, 5$ and $\vec{V}_{CBCT}(i)$, $i = 1, 2, 3, \dots, 5$ in the experimental coordinate system, which is defined to be the same as the laboratory coordinate system, and rotation in the 3D space is denoted as:

$$R_3(\alpha, \beta, \gamma) = \begin{bmatrix} \cos \beta \cos \gamma - \sin \alpha \sin \beta \sin \gamma & \sin \beta \sin \gamma + \sin \alpha \sin \beta \cos \gamma & -\cos \alpha \sin \beta \\ -\cos \alpha \sin \gamma & \cos \alpha \cos \gamma & \sin \alpha \\ \sin \beta \cos \gamma + \sin \alpha \cos \beta \sin \gamma & \sin \beta \sin \gamma - \sin \alpha \cos \beta \cos \gamma & \cos \alpha \cos \beta \end{bmatrix} \quad (1)$$

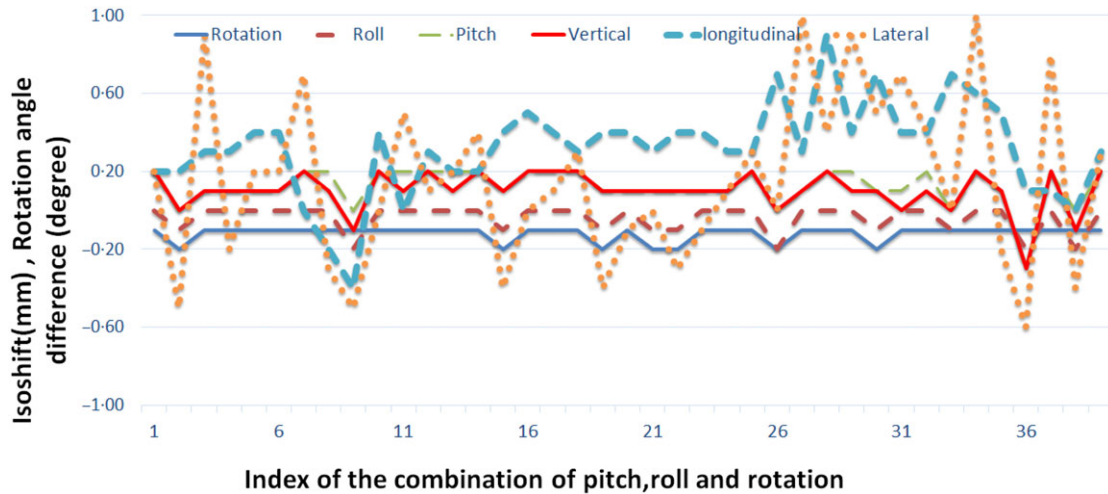


Figure 2. The isocentre translation shifts for different combinations of pitch, roll and yaw by Vision RT, and the rotation angle differences between Vision RT and console input for different combinations of pitch, roll and yaw.

and translation is

$$T_3(X_T, Y_T, Z_T) = \begin{bmatrix} -X_T \\ -Y_T \\ -Z_T \end{bmatrix} \quad (2)$$

Then CBCT images and CT images are related through the following equation:

$$\vec{V}_{3CBCT}(i) = R_3 \vec{V}_{3CT}(i) + T_3(X_T, Y_T, Z_T) \text{ for } i = 1, \dots, N \quad (3)$$

where $\vec{V}_{3CBCT}(i)$ and $\vec{V}_{3CT}(i)$ are the position vectors of a point in three-dimensional space.

Calculation of the rotation errors

In CBCT images of the SRS phantom, the rotational angles of pitch, roll and yaw for the five BBs were assumed to be α , β and ν , respectively. Following the suggestion in Ref. 18, the ‘CBCT image’ at neutral position was used to replace the planning CT image in the image registration.

$V_{3CBCT}(i)_{\alpha=\beta=\nu=0}$ is the i -th BB position of the CBCT images taken at neutral position. With known rotation angles α , β and ν , the i -th BB position should be $\vec{V}_{3CBCT}(i)$ which is $R_3(\alpha, \beta, \nu) V_{3CBCT}(i)_{\alpha=\beta=\nu=0} + T_3$, and T_3 is the couch translation motion caused by the couch rotation.

A linear least square fit method was used to determine the rotations and translations.^{18,28}

In this method, a solution of R_3 and T_3 would be found such that

$$\sum_{i=1}^N |\vec{V}_{3CBCT}(i) - R_3 \vec{V}_{3CT}(i) - T_3|^2 \quad (4)$$

reaches a minimum for all N points; thus, the difference between observation and expectation is minimal. It can be examined that the corresponding solutions are Eq. (5) and Eq. (6)^{38,39}:

$$T_3 = \frac{\sum_{i=1}^N \vec{V}_{3CBCT}(i)}{N} - R_3 \frac{\sum_{i=1}^N \vec{V}_{3CT}(i)}{N} \quad (5)$$

and

$$R_3 = USV^T \quad (6)$$

with

$$\frac{1}{N} \sum_{i=1}^N \left(\vec{V}_{3CBCT}(i) - \frac{\sum_{i=1}^N \vec{V}_{3CBCT}(i)}{N} \right) \left(\vec{V}_{3CT} - \frac{\sum_{i=1}^N \vec{V}_{3CT}(i)}{N} \right)^T = UDV^T. \quad (7)$$

Here, UDV^T is the singular value decomposition of the matrix, and the detail information can be found in Refs. 38 and 39, D is a diagonal matrix. S is also a diagonal matrix which is determined by U and V .^{38,39} Once the matrix R_3 is determined, so are the rotational angles. The differences between these rotation angles and the inputs from the console were defined as the uncertainties of the rotational angles. The translation of the central BB was calculated and represented the isocentre shift of the couch during the rotation. Detailed derivations of Eq. (4) to Eqs (5) and (6) can be found in Ref. 38, and the explanation of the singular value decomposition method can be found in Ref. 39.

In our data analyses, 15 equations were used to determine 6 parameters of the rotation and translation. The number of the equations was more than the number of variables. Thus, the system was an overdetermined system.

Results

Accuracy test of the proposed methodology

The following experiments were carried out with a uniformly distributed weight of 200 kg on the couch. Figure 2 shows the isocentre shifts for all 39 combinations of pitch, roll and rotation by using Vision RT. The maximum isocentre shifts were 0.8 mm in the X direction, 0.7 mm in the Y direction and -0.1 mm in the Z direction. The mean values and standard deviations were -0.16 ± 0.45 mm, 0.22 ± 0.24 mm and -0.02 ± 0.45 mm for X, Y and Z directions, respectively. The rotation angle differences between those Vision RT detected and the PerfectPitch couch

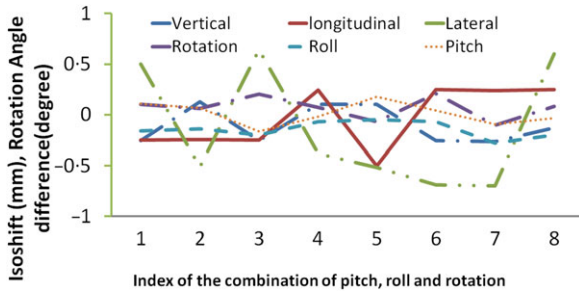


Figure 3. The translation shifts and residual rotation angles for all eight combinations of pitch, roll and yaw from the CBCT method.

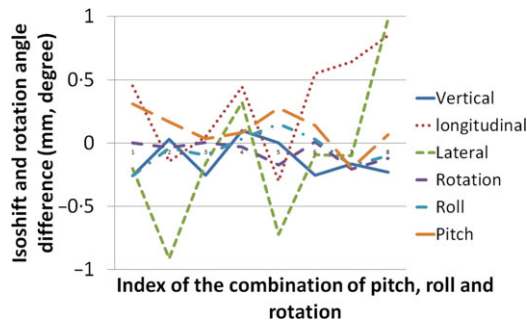


Figure 4. The translation shifts and residual rotation angles between Vision RT and CBCT for all eight combinations of pitch, roll and yaw.

programmed are also plotted in Figure 2. These differences represent the remaining rotational errors even after 6-DOF couch corrections. The maximum rotation angle differences were 0.2 degree for pitch, 0.1 degree for roll and -0.2 degree for couch rotation. The mean values and standard deviations were 0.16 ± 0.06 degree, 0.08 ± 0.06 degree and 0.12 ± 0.04 degree for pitch, roll and rotation, respectively. These angles are quite small and can be safely ignored in clinical applications.

For CBCT image study, because of its complex and time-consuming process, only those phantom CBCT images at the eight most allowed combinations of rotation, roll and pitch of the 6-DOF couch were acquired and named as 1 to 8: (3,3,3), (3,357,3), (3,3,357), (3,357,357), (357,3,3), (357,357,3), (357,3,357) and (357,357,357). Those represent the most allowed cases in clinical practice and should be enough for this study. The CBCT image registration results are shown in Figure 3. The results are similar to those of the Vision RT image method.

The differences between Vision RT and CBCT results are given in Figure 4 for the eight most allowed combinations of rotation, roll and pitch. It is clear that the rotation angle differences between Vision RT and CBCT are less than 0.3 degree, and the translation errors are less than 1 mm. Thus, Vision RT is accurate for application in the patient pre-set-up and monitoring during patient treatments.

Conclusions

To verify the accuracy of 6-DOF couch, a total of 39 combinations of pitch, yaw and roll rotations of an SRS phantom were evaluated by using Vision RT system. This evaluation was done with a weight of 200 kg on couch. The uncertainties of rotation and translation were estimated.

CBCT images of the SRS phantom were acquired under a total of eight extreme conditions of rotation. An in-house software was used to detect the five BBs inside the phantom and register those BBs to calculate rotation. The accuracy between CBCT and Vision RT were also compared for the eight cases. It was observed that the results from those two methods are in good agreement.

All shifts of isocentre caused by residual rotation errors were less than 1 mm and considered clinically insignificant for the majority of radiotherapy treatments where the set-up margins are generally bigger than 3 mm. The applied margins for SRS cases are varied from one institution to another. From our clinical experience, the evaluated couch and imaging guidance systems can be safely used for the cases where the CTV to PTV margins are around or bigger than 2 mm.

Financial Support. No funding.

Conflict of Interest. No conflict of interest.

References

- Roper J, Chanyavanich V, Betzel G, Switchenko J, Dhakaan A. Single Isocenter multiple target stereotactic radiosurgery: risk of compromised coverage. *Int J Radiat Oncol Biol Phys.* 2015; 93(3): 540–546.
- Zhang Q, Song Y, Chan M, Burman C, Yamada Y. Feasibility study of real time planning for stereotactic radiosurgery. *Med Phys.* 2013; 40(3): 031711.
- Lee J, Kim J, Ye S, Kim H, Carlson J, Min J. Dosimetric effects of roll rotational setup errors on lung stereotactic ablative radiotherapy using volumetric modulated arc therapy. *Br J Radiol.* 2015; 88: 20140862.
- Cao M, Laley F, Das I, DesRosiers C, Slessinger E, Cardenes H. Evaluation of rotational errors in treatment setup of stereotactic body radiation therapy of liver cancer. *Int J Radiat Oncol Biol Phys.* 2012; 84: e435–e440.
- Amro H, Hamstra D, Mcshan D, Sandler H, Vinberg K, Hadley S and Litzenberg D. The dosimetric impact of prostate rotations during electromagnetic guided external beam radiation therapy. *Int J Radiat Oncol Biol Phys.* 2013; 85: 230–236.
- Zhang Q, Xiong W, Chan M, Song Y and Burman C. Rotation effects on the target volume margin determination. *Phys Med.* 2015; 31: 80–84.
- Mageras GS, Fuks Z, Leibel SA, Ling CC, Zelefsky MJ, Kooy HM, van Herk M and Kutcher G J. Computerized design of target margins for treatment uncertainties in conformal radiotherapy. *Int J Radiat Oncol Biol Phys.* 1999; 43: 437–445.
- van Herk M, Remeijer P, Rasch C, Lebesque J. The probability of correct target dosage: dose-population histograms for deriving treatment margins in radiotherapy. *Int J Radiat Oncol Biol Phys.* 2000; 47: 1121–1135.
- Yan D, Lockman D, Martinez A, Wong J, Brabbins D, Vicini F, Liang J, Kestin L. Computed tomography guided management of interfractional patient variation. *Semin Radiat Oncol.* 2005; 15: 168–179.
- Yue N, Knisely J, Song H, Nath R. A method to implement full six-degree target shift corrections for rigid body in image-guided radiotherapy. *Med Phys.* 2005; 33: 21.
- Jin J Y, Yin F F, Tenn S, Medin P, Solberg T. Use of the BrainLab ExacTrac X-Ray 6D system in image guided radiotherapy. *Med Dosim.* 2008; 3: 124–134.
- Takakura T, Mizowaki T, Nakata M, Yano S, Fujimoto T, Miyabe Y, Nakamura M, Hiraoka M. The geometric accuracy of frameless stereotactic radiosurgery using a 6D robotic couch system. *Phys Med Biol.* 2010; 55: 1–10.
- Chang Z, Wang Z, Ma J, O'Daniel J C, Kirkpatrick J, Yin F. 6D Image guidance for spinal non-invasive stereotactic body radiation therapy: comparison between ExacTrac X-ray 6D with kilo-voltage cone-beam CT. *Radiation Oncol.* 2010; 95: 116–121.
- Meyer J, Wilbert J, Baier K, Guckenberger M, Richter A, Sauer O, Flentje M. Positioning accuracy of Cone-beam computed tomography in combination with a HexaPOD robot treatment table. *Int J Radiat Oncol Biol Phys.* 2007; 67: 1220–1228.

15. Gevaert T, Verellen D, Engels B, Depuydt T, Heuninckx K, Duchateau M, Reynders T, De Ridder M. Clinical evaluation of a robotic 6-degree of freedom treatment couch for frameless radiosurgery. *Int J Radiat Oncol Biol Phys.* 2012; 83: 467–474.
16. Guckenberger M, Meyer J, Wilbert J, Baier K, Sauer O, Flentje M. Precision of image guided radiotherapy (IGRT) in six degree of freedom and limitations in clinical practice. *Strahlenther Onkol.* 2007; 183: 207–310.
17. Schmidhalter D, Fix M K, Wyss M, Schaer N, Munro P, Scheib S, Kunz P, Manser P. Evaluation of a new six degree of freedom couch for radiation therapy. *Med Phys.* 2013; 40(11): 111710.
18. Zhang Q, Driewer J, Wang S, Li S, Zhu X, Zheng D, Cao Y, Zhang J, Jamshidi A, Cox B, Knisely J, Potters L, Klein E. Accuracy evaluation of a six degree of freedom couch using cone beam CT and IsoCal Phantom with an in-house algorithm. *Med Phys.* 2017; 44(8): 3888–3898.
19. Chan M, Lim S, Li X, Tang X, Zhang P, Shi C. Commissioning and evaluation of a third party six degree of freedom couch used in radiotherapy. *Technol Cancer Res Treat.* 2019. doi: [10.1177/1533033819870778](https://doi.org/10.1177/1533033819870778)
20. Fu C, Ma C, Shang D, Qiu Q, Meng H, Duan J, Yin Y. Geometric accuracy evaluation of a six-degree-of-freedom (6-DoF) couch with cone beam computed tomography (CBCT) using a phantom and correlation study of the position errors in pelvic tumor radiotherapy. *Transl Cancer Res.* 2020; 9(10): 6005. doi: [10.21037/tcr-20-1528](https://doi.org/10.21037/tcr-20-1528)
21. Froseth T C, Strickert T, Solli K, Salvesen O, Frykholm G, Reidunsdatter R. A randomized study of the effect of patient position on setup reproducibility and dose distribution to organs at risk in radiotherapy of rectal cancer patients. *Radiat Oncol.* 2015; 10: 217.
22. McBain C, Henry A, Sykes J, Amer A, Marchant T, Moore C, Davies J, Stratford J, McCarthy C, Porritt B, Williams P, Khoo V, Price P. X-ray volumetric imaging in image-guided radiotherapy: the new standard in on-treatment imaging. *Int J Radiat Oncol Biol Phys.* 2006; 64: 625–634.
23. Jaffray D A, Siewerdsen J H, Wong J W, Martinez A A. Flat-panel cone-beam computed tomography for image-guided radiation therapy. *Int J Radiat Oncol Biol Phys.* 2002; 53: 1337–1349.
24. Zheng D, Lu J, Jefferson A, Zhang C, Sleeman W, Weiss E, Dogan N, Song S, Williamson J. A protocol to extend the longitudinal coverage of on-board cone-beam CT. *J Appl Clin Med Phys.* 2012; 13: 141–152.
25. Xu Y, Yan H, Ouyang L, Wang J, Zhou L, Cervino L, Jiang S, Jia X. A method for volumetric imaging in radiotherapy using single x-ray projection. *Med Phys.* 2015; 42: 2493.
26. Cervino L, Pawlicki T, Lawson J D, Jiang S B. Frame-less and mask less cranial stereotactic radiosurgery: a feasibility study. *Phys Med Biol.* 2010; 55(7): 1863–1873.
27. Li G, Ballangrud A, Kuo L C, Kang H, JKirov A, Lovelock M, Yamada Y, Mechalakos J, Amols H. Motion monitoring for cranial frameless stereotactic radiosurgery using video based three dimensional optical surface imaging. *Med Phys.* 2011; 38(7): 3981–3994.
28. Li G, Wei J, Huang H, Chen Q, Gaebler C P, Lin T, Yuan A, Rimner A, Mechalakos J. Characterization of optical surface imaging based spirometry for respiratory surrogating in radiotherapy. *Med Phys.* 2016; 43(3): 1348–1360.
29. Li G, Lovelock D M, Mechalakos J, Shyam R, Della-Biancia C, Howard A, Nancy L. Migration from full-head mask to open face mask for immobilization of patients with head and neck cancer. *J Appl Clin Med Phys.* 2013; 14: 243–254.
30. Kang H, Patel R, Roeske J. Efficient quality assurance method with automated data acquisition of a single phantom setup to determine radiation and imaging isocenter congruence. *J Appl Clin Med Phys.* 2019; 20(10): 127–133.
31. Tang X, Cullip T, Dooley J, Zagar T, Jones E, Chang S, Zhu X, Lian J, Marks L. Dosimetric effects due to the motion during deep inspiration breath hold left-sided breast cancer radiotherapy. *J Appl Clin Med Phys.* 2015; 16(4): 91–99.
32. Scheffel P J, Harms W, Sroka-Perez G, Schlegel W, Karger C P. Accuracy of a commercial optical 3D surface imaging system for realignment of patients for radiotherapy of the thorax. *Phys Med Biol.* 2007; 52(13): 3949–3963.
33. Bergom C, Currey A, Desai N, Tai A, Strauss J B. Deep inspiration breath hold: techniques and advantages for cardiac sparing during breast cancer irradiation. *Front Oncol.* 2018; 8: 87.
34. Gao S, Du W, Balter P, Munro P, Jeung A. Evaluation of IsoCal geometric calibration system for Varian linacs equipped with on-board imager and electronic portal imaging device imaging systems. *J Appl Clin Med Phys.* 2014; 15(3): 4688.
35. Varian Truebeam Technical Reference Guide: Volume 2: Imaging, 2016, published by Varian Comapny.
36. Vision RT Calibration Phantom, 0002-0116, 2015, published by Vison RT Company.
37. Siddon R L. Solution to treatment planning problem using coordinate transformations. *Med Phys.* 1981; 8: 766.
38. Umeyama S. Least-squares estimation of transformation parameters between two point patterns. *IEEE Trans. Pattern Anal. Mach. Intell.* 1991; 13(4): 376–380.
39. Press W, Teukolsky S, Vetterling W, Flanenery B. *Numerical Recipes in C*: Cambridge University Press, 2002.